Improving the continuous photogrammetric monitoring system

M Amparo Núñez-Andrés [1], Albert Prades-Valls [2],

[1] Civil and environmental engineering department. Universitat Politècnica de Catalunya-BarcelonaTech, Barcelona, Spain - m.amparo.nunez@upc.edu
[2] Civil and environmental engineering department. Universitat Politècnica de Catalunya-BarcelonaTech, Barcelona, Spain - alberto.prades.i@upc.edu

Keywords: Monitoring, Digital Photogrammetry, Vegetation masks, Precursor movements, Rockfalls detection, Cross correlation

Abstract

The basalt wall next to the Fluvià river, where Castellfollit de la Roca (Girona) is located, is known for its high frequency of rockfalls, which can affect existing buildings. To monitor it, a continuous photogrammetry system developed by the UPC's geomatics engineering group and the ICGC was installed in 2021. This system, consisting of three cameras, has since captured images that are sent to the server located at the UPC, where they are processed to detect movements in the rock massif over time. If a rockfall is detected, a three-dimensional model is generated to estimate the volume of rock mobilised.
This massif is characterised by the presence of changing vegetation and a high frequency of rainy and foggy days. These changes in the appearance of the rockfall decrease the sensitivity of the photographic system to the detection of premonitory movements or low-volume rockfalls. To mitigate these effects, improvements have been made to the matching algorithms. These improvements include the implementation of different procedures such as the automatic selection of the best quality daily image, radiance balancing techniques and the creation of dynamic masks adapted to vegetation changes.

1. Introduction

Among the various activities involved in risk management is the anticipation of rockfalls in order to be able to make decisions such as the assessment and inventory of incidents for their characterisation. In this area, monitoring systems play an important role (Janeras et al., 2016; Blanch et al., 2021), with a double objective. On the one hand, the detection of possible premonitory movements prior to the fall of rocky blocks. On the other hand, the identification of areas where a rockfall has occurred, which need not have been previously identified as active areas with previous movements.

This type of monitoring can only be carried out with continuous measurement systems or with very high frequency campaigns, making the latter option unfeasible due to the high consumption of time and resources in travel. In the case study presented in Castellfollit de la Roca (Girona, Spain), a photographic continuous measurement system was designed and installed with three fixed cameras that take images at regular intervals predetermined by the user (Matas et al., 2022). Unlike the work developed by other authors (Kromer et al., 2019; Blanch et al., 2021), changes are not identified on the 3D model generated from the images, but on the images themselves similar to the process follows in Desrues eta l, (2019).

This system has been operational from mid-June 2021 to the present, with minor interruptions due to mechanical or connection issues, both the connection and the mechanical part of one of the cameras. The model chose was a Canon EOS 6D Mark II model, which has a CMOS-type sensor with a 3/2 ratio, a size of 35.9 × 24.0 mm, resolution of up to 6240 × 4160 pixels, and a 105 mm focal length. Fixed photographic conditions were used to take the photographs, such as sensitivity at ISO 100 and an aperture of f/8, to leave the calculation of the exposure time based on the fixed variables and the reading of the camera's photometer. The GSD (Ground Sample Distance) was about 1 cm, since the distance between the cameras and the wall was approximately 170 m. The distance between cameras is about 35 m.

From the beginning, the system was not without difficulties, some of them unexpected. For example, the cameras, despite being on fixed supports (Figure 1), suffer from sub-millimetric changes in their position due to vibration caused by wind or by the minute displacements of the supports due to temperature changes throughout the day. Exceptionally, larger movements occur. For example, in February 2023, one of the cameras broke down and had to be taken apart to repair it. When it was reassembled, it was not in exactly the same position as before Most of the time these movements cause shifts of only a few pixels in the images and occasionally they can shift a few tens of pixels. In any case, it is necessary to reference them against each other before starting the matching algorithms. It must be considered that the referencing will always be with respect to the image that was taken as the standard in each multi-temporal analysis.

Figure 1. Cameras and control system

On the other hand, the study area is highly complex, as it is covered by seasonally changing vegetation. It is an area of high rainfall and the Fluviá river flows through the foot of the massif, which tends to produce fog, especially during the autumn and winter months (Figure 2 down). The massif under study is oriented to the north and due to the relative location of the cameras there are usually problems of poor lighting due to backlighting. All these changing elements over time complicate and diminish the sensitivity of the system to the detection of subtle premonitory movements, of millimetric or centimetric order, which can occur, sometimes for months, before a block detachment.

The multi-temporal analysis, independent for each of the cameras, is carried out using cross-correlation once the images have been registered. In order to improve the results obtained so far, the following changes have been introduced to the original solution:

- A previous analysis of the quality of the images to automatically eliminate those that are not useful.
- Techniques to balance and equalise radiance.
- Creation of dynamic masks that adapt to seasonal changes in vegetation.

Figure 2. Up: seasonal vegetation changes. Down: image in a foggy day.

2. Study area

The study area is located in the municipality of Castellfollit de la Roca (Catalonia, Spain) at an altitude of 296 m above sea level. Part of the town centre sits on a basaltic cliff about 50 m high and a perimeter of about one kilometre. The rivers Fluvià, to the north of the massif, and Toronell, on the south side, run around the cliff face and are the cause of the erosive action. In this cliff there are prismatic disjunctions that form when the basalt cools slowly. Due to erosion, these basalt columns can generally collapse after a toppling failure. Because of the location of the village on the massif, some building are in the edge of the cliff, monitoring studies have been carried out in the area for some time. Previous observations with laser-scanning instrumentation (Terrestrial Laser System-TLS) detected precursor deformations to block detachment (Abellan et al., 2011) with displacements of less than 1.7 cm per year.

3. Methodology

In this section we will detail the process followed to improve each of the points highlighted in section 1. These operations must be carried out before registering the images and proceeding to apply the cross-correlation algorithms.

To perform the adjustment, the system locates homologous points in both images. This process cannot be performed correctly if the quality of the images is not adequate, as the identification of these points becomes difficult.
The following sections detail the preparation of the images before the multi-temporal analysis for the detection of movements and changes on the images.

3.1 Quality image assessment

In order to analyse the quality of the images to be used for the multi-temporal analysis, two parameters have been tested with varying degrees of complexity in their implementation: the mean square value of the Laplacian and the analysis of the presence of high frequencies in the Fourier transform spectrum.

The Laplacian is an operator that measures the second spatial derivative of an image, which can be thought of as the local rate of change of the image intensity. The variance of the Laplacian measures the local variation of the intensity, which can be useful for detecting areas of abrupt changes in the image. If the Laplacian variance is high, then the image may have areas with edges or important details, whereas, if it is low, it may indicate a blurred or smoothed image. Therefore, the Laplacian variance can be a good indicator of the sharpness or clarity of an image. This parameter is also known as the focus index.

The application of the Discrete Fourier Transform (DFT) to a digital image allows its frequency spectrum to be obtained. This can provide valuable information about the image, such as the amplitude and the potential drop at the dominant frequencies. The amplitude refers to the intensity of the signal at a given frequency, while the power drop refers to how fast the intensity decreases as the frequency increases.

Also, a well-defined image will have information in a wide range of frequencies, from low frequencies to high frequencies, while a blurred, low-quality image will have a more limited frequency distribution, especially a strong loss in the high frequencies. In other words, a high-quality image will contain fine details and high frequency textures, while a low-quality image will lack these details. The process followed is to fit a potential function, ec (1), to the frequency spectrum.

$$y = A\,x^{-a} \qquad (1)$$

This allows us to determine the multiplicative parameter A which is linked to the general illumination of the scene and, most importantly for our study, the potential parameter a which indicates the rate of fall of the frequency spectrum. If the function drops very quickly, it means that there is no presence of high frequencies, which occurs in images with little detail. In our case, it corresponds to images blurred by the presence of fog. If the function drops slowly, it means that the image contains high frequencies, i.e. it is sharp and the details of the object are perfectly defined.

https://doi.org/10.5194/isprs-archives-XLVIII-1-W4-2025-89-2025 | © Author(s) 2025. CC BY 4.0 License.

3.2 Quality image improvement

One way to improve the images both for comparison and for the identification of vegetation and the creation of masks, will be the improvement of the radiance balance.

For this purpose, a shift from the RGB colour space to the LAB colour space (Reinhard, 2001) has been applied. This colour space aims to linearize the colour transformation, i.e. to consistently relate numerical colour values to human visual perception. This property makes it suitable for comparisons of change between two images of the same location, even if the lighting conditions have changed.
In this new space, mean values (μ) and standard deviations (σ) are calculated for each channel of the two images. The image with the best illumination (*ref*) is taken as reference, and the digital levels of the worst illuminated image (*obj*) are transformed to equal the two statistics of the first one. This process is expressed from the expressions (2).

$$
\begin{aligned}
L_{obj_f} &= \left[\left(L_{obj} - \mu L_{obj} \right) \frac{\sigma L_{obj}}{\sigma L_{ref}} \right] + \mu L_{ref} \\
L_{obj_f} &= \left[\left(L_{obj} - \mu L_{obj} \right) \frac{\sigma L_{obj}}{\sigma L_{ref}} \right] + \mu L_{ref} \\
L_{obj_f} &= \left[\left(L_{obj} - \mu L_{obj} \right) \frac{\sigma L_{obj}}{\sigma L_{ref}} \right] + \mu L_{ref}
\end{aligned} \tag{2}
$$

Subsequently, the resulting image is returned to RGB space, correcting the radiometric differences with respect to the first image. These corrected images will be the basis for obtaining the vegetation masks, as the different colours are much more highlighted.

3.3 Use of vegetation masks

In the first analyses reported in (Núñez-Andrés et al., 2023a), a mask was used for vegetation that remained constant, regardless of the date of shooting. But after seeing the large variation, not only seasonal, it was considered necessary to create dynamic masks. That is to say, instead of creating a mask to be used during a period of time, one will be created for each image at the moment of its pre-processing. For this purpose, a combination of RGB filters on image and morphometric filters is used (Núñez-Andrés et al., 2021; Núñez-Andrés et al., 2023b).

The masks eliminate areas with vigorous vegetation so that most of the detection of non-rock wall movements is eliminated. Figure 3 shows on the top image a typical scene from the month of May, with large areas covered by vegetation. The bottom image shows the same image with the vegetation mask overlaid in green.

Among the different RGB filters tested (Anders et al., 2020), the GLI (Green Leaf Index), Ec 3, was the one that gave the best results in all cases, with the use of morphometric opening and closing. The GLI index provides a value resulted of highlighting the green areas. Negative values will show bare soils, water bodies and anthropic infrastructures. On the contrary, positive values will identify the presence of your vegetation through a colour gradient analogous to NDVI.

$$
GLI = \frac{(G - R) + (G - B)}{2G + R + B} \tag{3}
$$

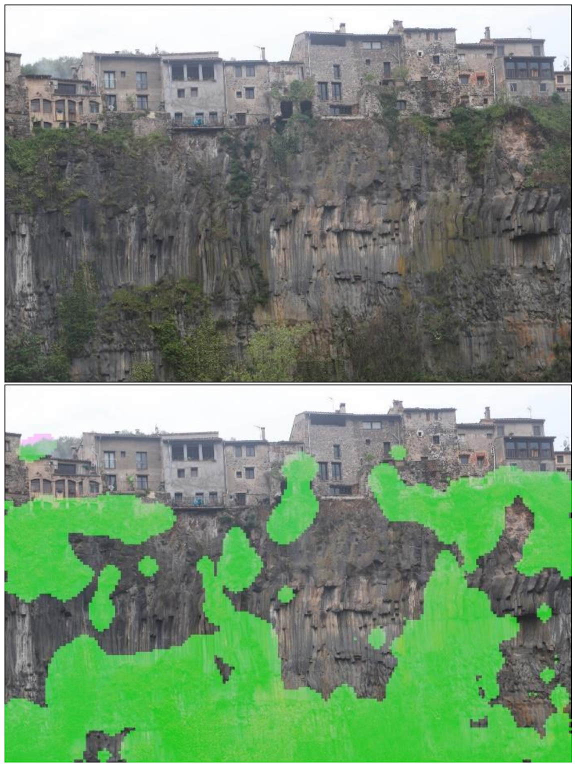

Figure 3. Top: image of a typical scene from the month of May, Bottom: the same image with the vegetation mask overlaid.

In these masked areas the change or movement detection algorithms will not be applied. However, there are still some areas with vegetation that, depending on the season, appear dry and are not detected by the GLI filter. This is one of the areas where further work needs to be done to improve in the future.

4. Results

4.1 Improvement results

To compare the results obtained by applying the Fourier transform or the Laplacian, we have chosen 3 images of varying quality, Figure 4, due to the fog and light conditions. We have obtained the parameters above mentioned in order to determine the quality of them to choose the best one for the movement's detection. Table 1 contains the size of each of the images and the parameters obtained in the analysis by both methods.

Figure 4. Representative images of the different quality obtained depending on environmental and sunlight conditions

https://doi.org/10.5194/isprs-archives-XLVIII-1-W4-2025-89-2025 | © Author(s) 2025. CC BY 4.0 License.

It was found that the images of poorer quality, in addition to having a smaller size because they are more compressed due to lack of contrast, correspond to much lower focus indices obtained from the Laplacian, between 11 and 12 times lower, than those of higher quality, on the left in figure 3, without any doubt. This image has a focus index of 56.2 and the worst one, the image on the right in Figure 4, of 4.7. With regard to the parameters obtained from the adjustment of a potential function to the frequency spectrum, it is found that the more defined images correspond to a lower power, indicating that the fall of the function is slower, which indicates the presence of high frequencies.

Image	Storage (MB)	Focus index	Amplitude	Exponent
Left	9.6	56.2	10.2	0.64
Centre	5.9	14.9	9.2	0.70
Right	4.9	4.7	9.2	0.99

Table 1. Results obtained after the quality analysis of the three images shown in Figure 3.

The use of the change of colour space to balance the radiance has allowed us to improve the contrast in the images and to highlight the vegetation zones, facilitating the creation of vegetation masks. At this point we have encountered a drawback, as the areas with moss on the columns are also highlighted. As mentioned above, this is an open line of work to try to avoid it, surely the solution is to combine different methodologies to obtain the final mask. Another drawback is that it has not been possible to detect the vegetation that has dried and therefore only remains as a set of grayish branches.

4.2 Volume and movements detection

The last step is to compare two images separated in time. For this, two algorithms have been implemented, one of them calculates the displacements of small portions of the image, which we will call pattern, by correlation with respect to the second image, ec (4), which we will call search. In the areas of the image where there are no movements, the correlation between the image portions will be close to unity and the measured displacement will be zero.

$$\rho(j,k) = \frac{\sum_{x=1}^{N}\sum_{y=1}^{M}\left[\left(I_c(x,y)-\bar{I}_c\right)\left(I_p(x,y)-\bar{I}_p\right)\right]}{\sqrt{\sum_{x=1}^{N}\sum_{x=1}^{N}\left(I_c(x,y)-\bar{I}_{cp}\right)^2}\sqrt{\sum_{x=1}^{N}\sum_{x=1}^{N}\left(I_p(x,y)-\bar{I}_p\right)^2}} \tag{4}$$

where ρ is the correlation value,
I_c and I_p are the radiometric levels of each area,
$\underline{Ic}$ and $\underline{Ip}$ are the average of the radiometric level in the pattern and adjustment windows and
(x, y) refers to each pixel of the matrix.

If any of the rock blocks shows a movement over time, the algorithm will signal a relative displacement between the image slices. If we do not use vegetation masks, not only will false positives be detected by the change in vegetation mass, but also the process will be slowed down.

We have detected two precursor movements in areas 1 and 2, Figure 5, of 40 cm and 20 cm before the detachment in May 2022 and August 2023 respectively. On areas 3 and 4 the detachment in May 2023 and August 2023 was without any precursor movement. The area 4 has different characteristics since it was rock without column structure.

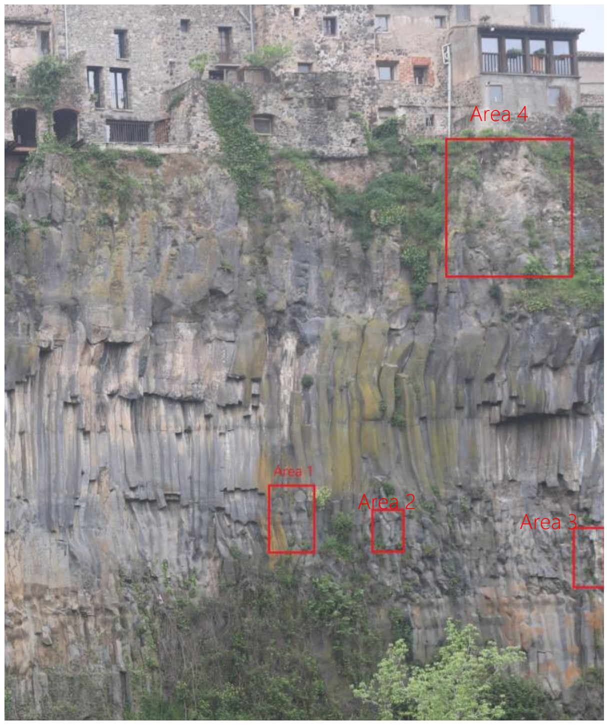

Figure 5. Different areas where movements or detachments have been detected between July 2021 and May 2025.

Figure 6 shows the latest detected movement. This portion of the image shows the displacement vectors of some of the rocks in the wall. Knowing that the size of a pixel corresponds to approximately one centimetre on the ground, the displacements that can be seen in the image range from 1 to 6 cm.

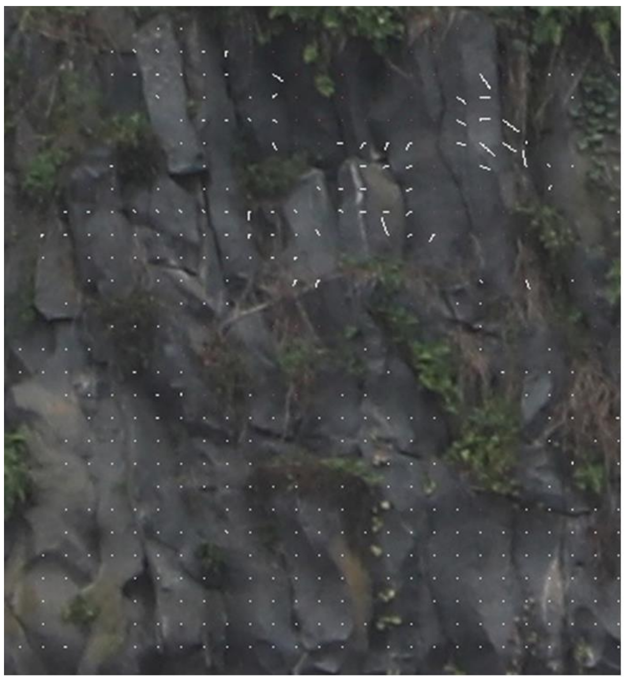

Figure 6. Vectors of movement obtained by image correlation.

The geometry of the system allows us to assume that, although we are in a projection, when working on a single 2D image, for camera 2, which is practically perpendicular to the analysed rock wall, a displacement of 1 pixel is equivalent to a displacement of the GSD of the image, i.e. 1 cm.

The second algorithm compares local correlations between images within a certain window of varying size. It is expected that in unchanged areas the local correlations will be close to unity and in areas where changes have occurred the local correlations will have lower values or close to zero. Figure 7 shows in red the area where a change has been detected due to the fall of a mass in May 2023.

The upper left image on Figure 7 was taken on May 11, 2023, at 7:30, and the one on the right is from May 13 at the same time. Below is the colour map that encodes the comparison based on the correlation value. Blue indicates that no changes have been detected, while red indicates that some change has been detected in the area. The bottom right image is a zoomed-in view of the area outlined in orange.

After the detection we can build the three model, from the images of the three cameras, in order to compute the volume. We can notice that the geometry of

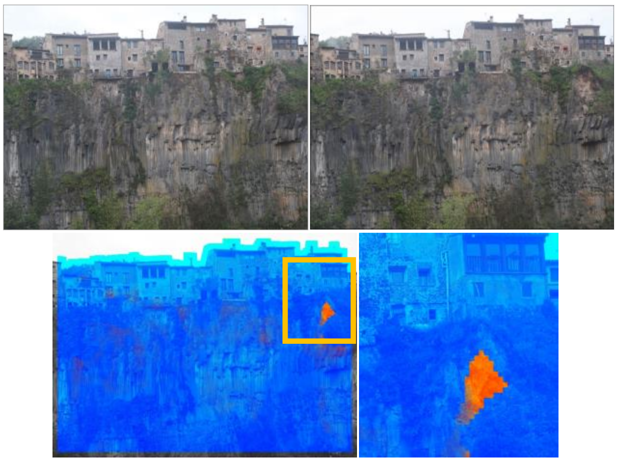

Figure 7. Detection of the detachment between 11 and 13 of May in 2023. Red area shows the zone where the part of the rocky wall falls.

5. Conclusions

The objective of a continuous monitoring system is to detect premonitory movements in a rock face that give early warning of future rock falls. In the event that a rockfall occurs, the focus shifts to calculating the volume of rock that has broken off. This system can improve the early warning methods for rockfalls and, on the other hand, contributes to know the magnitude-frequency relationship of the monitored wall, information that will help to improve the quantitative analysis of the risk.

To avoid false alarms, it is necessary to have quality images and to eliminate any movement that does not correspond to the rocky blocks.

In the present work, three objectives have been set to improve the automation of the processes. The three steps are the estimation of the quality of the images, elimination of those that do not exceed the imposed minimum quality criteria and the creation of dynamic masks to eliminate areas with vegetation.
With its implementation, the existing workflow has been improved to increase the system's ability to detect possible precursor movements prior to the fall of the rock blocks. The identification of images that have a higher quality automatically, as well as the radiance correction have been successfully completed, and some significant parameters have been defined to determine the quality. In the case of vegetation masks, although the results are satisfactory in most cases, further work is needed to identify those situations in which moss is identified and therefore a significant percentage of the area of interest is eliminated from the analysis.

The improvements implemented have allowed a more accurate multitemporal analysis avoiding false positives. In addition, it allows us to reduce the image processing time.

Acknowledgements

Part of this research was funded by project Georisk, “Advances in rockfall quantitative risk analysis (QRA) incorporating developments in geomatics (GeoRisk)”, grant number PID2019-103974RB-I00, funded by MCIN/AEI/10.13039/501100011033, the Ministerio de Ciencia e Innovación and the Agencia Estatal de Investigación of Spain.

References

Abellan A., Vilaplana J. M., Calvet J., García-Sellés D., and Asens E. 2011: Rockfall monitoring by Terrestrial Laser Scanning - Case study of the basaltic rock face at Castellfollit de la Roca (Catalonia, Spain). *Natural Hazards and Earth System Sciences* 11(3), pp. 829-841. https://doi.org/10.5194/nhess-11-829-2011

Anders, N., Valente, J., Masselink, R., Keesstra, S. 2019: Comparing Filtering Techniques for Removing Vegetation from Uav-Based Photogrammetric Point Clouds. *Drones*, 3(3), 61; https://doi.org/10.3390/drones3030061

Blanch X., Eltner A., Guinau M. and Abellan A. 2021: Multi-Epoch and Multi-Imagery (MEMI) Photogrammetric Workflow for Enhanced Change Detection Using Time-Lapse Cameras. *Remote Sens.* 13, 1460. https://doi.org/10.3390/rs13081460

Desrues, M.; Malet, J.P.; Brenguier, O.; Point, J.; Stumpf, A.; Lorier, L. 2019: TSM-Tracing Surface Motion: A Generic Toolbox for Analyzing Ground-Based Image Time Series of Slope Deformation. *Remote Sens.*, 11, 2189. https://doi.org/10.3390/rs11192189

Janeras, M., Jara, J.A., Royán, M.J., Vilaplana, J.M.,Aguasca, A., Fàbregas, X., Gili, J.A., and Buxó, P. 2016: Multi-technique approach to rockfall monitoring in the Montserrat massif (Catalonia, NE Spain), *Eng. Geol.*, https://doi.org/10.1016/j.enggeo.2016.12.010

Kromer, R., Walton, G., Gray, B., Lato, M., Group, R. 2019: Development and Optimization of an Automated Fixed-Location Time Lapse Photogrammetric Rock Slope Monitoring System. *Remote Sen. 11(16),* 1890; https://doi.org/10.3390/rs11161890

Matas G, Prades A, Núñez-Andrés MA, Buill F, Lantada N. 2022: Implementation of a fixed-location time lapse photogrammetric rock slope monitoring system in Castellfollit de la Roca, Spain. In: *5th Joint International Symposium on Deformation Monitoring (JISDM 2022*), Valencia, April 6-8 of 2022.

Núñez-Andrés, M.A., Prades, A., Matas, G., Buill, F., Lantada, N. 2023: New approach for photogrammetric rock slope premonitory movements monitoring. *Remote sen.*. 15 (2), 293. https://doi.org/10.3390/rs15020293

Núñez-Andrés, M.A., Prades, A., & Buill, F. 2021: Vegetation Filtering using Colour for Monitoring Applications from Photogrammetric Data. En: GISTAM 2021. https://doi.org/10.5220/0010523300980104

Núñez-Andrés, M.A.; Buill, F.; Prades, A. 2023: Geomatic techniques to filter vegetation from point clouds. En: *International Journal of Civil and Architectural Engineering*, vol. 17, no. 10, 2023.. ISBN/ISSN: 1307-6892. https://publications.waset.org/abstracts/civil-and-architectural-engineering

Reinhard, E., Adhikhmin, M., Gooch, B. T., & Shirley, P. 2001: Color transfer between images. IEEE Computer Graphics and Applications, 21(4), 34-41. https://doi.org/10.1109/38.946629